Available online at www.sciencedirect.com
SCIENCE DIRECT®
Chemical Physics Letters 407 (2005) 217–221
CHEMICAL PHYSICS LETTERS
www.elsevier.com/locate/cplett

Time-resolved kinetic studies on quenching of C_2 ($d^3\Pi_g$) by alkanes and substituted methane molecules

Hailing Wang, Zhiqiang Zhu, Shaohua Zhang, Linsen Pei, Yang Chen *

Hefei National Laboratory for Physical Sciences at Microscale, Department of Chemical Physics, University of Science and Technology of China, Hefei, Anhui, 230026, PR China

Received 22 December 2004; in final form 17 February 2005
Available online 13 April 2005

Abstract

C_2 free radicals were produced by photolysis of selected precursors (C_2Cl_4) with the focused output from the fourth harmonic of a Nd: YAG laser at 266 nm. The generated C_2 ($a^3\Pi_u$) radicals were then electronically excited to the $d^3\Pi_g$ state with a Nd: YAG laser pumped dye laser at 516.5 nm in the (0,0) band of the C_2 ($d^3\Pi_g \leftarrow a^3\Pi_u$) transition. The rate constants k_q and averaged collision cross sections σ_q for collision quenching of C_2 ($d^3\Pi_g$) by n-C_nH_{2n+2} (n = 1–8) and $CH_{4-n}Cl_n$ (n = 2–4) were measured at room temperature (298 K) by time–resolved laser-induced fluorescence in cell at total pressure of about 15 Torr. Formation cross sections of complexes for the C_2 ($d^3\Pi_g$) and quenchers were calculated by means of a collision complex model. It was shown that the quenching rates of C_2 ($d^3\Pi_g$) by alkane molecules increase with the number of C–H bonds of the molecules, which is in agree with that of the measured quenching cross sections.

1. Introduction

C_2 free radical is found in a very wide source, which occurs in comets, interstellar and in stellar atmosphere. It plays an important role in astrophysics as well as in many combustion systems where C_2 is present in large concentration [1–4]. In the last decades, there has been great progress in understanding some aspects of C_2 ($X^1\Sigma_g^+$) and C_2 ($a^3\Pi_u$) reaction kinetics. Reisler, Mangir and Wittig (RMW) [5–9] made observations on the reactions of both C_2 ($X^1\Sigma_g^+$) and C_2 ($a^3\Pi_u$) with NO, O_2, vinyl cyanide and ethylene. Some rate coefficients for the removal of C_2 ($X^1\Sigma_g^+ \& a^3\Pi_u$) and C_2 ($a^3\Pi_u$) $\leftrightarrow$ C_2 ($X^1\Sigma_g^+$) intersystem crossing were reported. Pesternack et al. [10–12] studied the reaction of C_2 ($a^3\Pi_u$) with hydrogen and small hydrocarbons. Fontijn's group studied the temperature dependence of the reactions of C_2 ($a^3\Pi_u$) with O_2 and NO in a high-temperature photochemistry reactor [13,14]. Kaiser et al. [15,16] studied the reaction of C_2 ($X^1\Sigma_g^+$) with H_2S and C_2H_4 under single collision conditions in crossed beam. Wang et al. [17,18] studied the reactions of C_2 ($a^3\Pi_u$) with H_2S and H_2O with ab initio calculations. Recently, our laboratory studied the kinetics of the C_2 ($a^3\Pi_u$) reactions with alkanes, some inorganic molecules and some small sulfur containing molecules by LIF [19–21]. Although quite an extensive set of data of the reactions of the ground state, C_2 ($X^1\Sigma_g^+$), and the metastable triplet state, C_2 ($a^3\Pi_u$), have hitherto been accumulated, there have been few investigations of the kinetics excited C_2 ($d^3\Pi_g$). In this Letter, the quenching rate constants of C_2 ($d^3\Pi_g$) by a rang of alkanes and substituted methane molecules were reported by the time-resolved laser-induced fluorescence of the C_2 ($d^3\Pi_g$) at room temperature and total pressure of about 15 Torr. Furthermore, formation cross sections of

* Corresponding author. Fax: +86 551 3607084.
E-mail address: yangchen@ustc.edu.cn (Y. Chen).

0009-2614/$ - see front matter © 2005 Elsevier B.V. All rights reserved.
doi:10.1016/j.cplett.2005.02.127

complexes for the C_2 ($d^3\Pi_g$) and quenchers were calculated by means of a collision complex model.

2. Experiment

The pulsed laser photolysis/laser-induced fluorescence (LP-LIF) experiments were performed in a stainless steel flow reactor in present work, which is basically similar to those described by other authors in literatures previously [22,23]. Briefly, triplet C_2 radicals were generated from the selected polyatomic molecules photolysis with the focused output from a fourth harmonic of a Nd: YAG laser (New wave) at 266 nm. The typical pulse energy and time jitter of the photolysis laser are 5 mJ and 2 ns. The C_2 molecules in the $a^3\Pi_u$ state were electronically excited to $d^3\Pi_g$ by a dye laser beam (Sirah) pumped by a Nd: YAG laser (Spectra physics, GCR-170, repetition rate of 10 Hz) with a pulse width of 8 ns and jitter 2 ns. The excitation laser passed collinear with and counters propagating to the photolysis beam. The dye laser was tuned to the (0,0) band of the C_2 ($d^3\Pi_g \leftarrow a^3\Pi_u$) transition at 516.5 nm. In order to minimize scatter light, the laser beams passed through a system of special light baffles. Emission fluorescence was monitored on the (0,1) band of the C_2 ($d^3\Pi_g \rightarrow a^3\Pi_u$) transition at 563.5 nm and collected by a lens system, passed through an interference filter (0.7 nm FWHM) and, then, focused into a photomultiplier (R928, Hamamatsu). The output of the photomultiplier was fed into a digital storage oscilloscope (TDS380, Tektronix) or a transient digitizer and then averaged with a computer data acquisition system. In our experiments, the fluorescence signals were averaged over 256 laser pulses.

In a typical experiment, a premixed gas sample containing a suitable polyatomic molecules as the C_2 radical precursor in Ar; the quencher mixed with Ar; and pure Ar as buffer gas, supplied from cylinders through stainless steel line and controlled by individually calibrated mass flow controller (D07-7A/2M, Beijing), is slowly passed through the fluorescence chamber. Typical precursor concentrations used were about 2.5×10^{14} molecule cm^{-3}. The quencher concentrations were varied in the range from 5×10^{14} molecule cm^{-3} up to 5×10^{15} molecule cm^{-3}. The total pressure in the chamber was bout 15 Torr. Under these conditions, the C_2 radicals are rotationally cooled to room temperature within 10 μs, and the diffusion times out of the observation area are >150 μs.

Gas sources and purities were: C_2Cl_4 (Shanghai, ⩾97%), CH_4 (Chengdu, 99.999%), C_2H_6 (Nanjing, 99.99%), C_3H_8 (Nanjing, 99.99%), C_4H_{10} (Nanjing, 99.99%), *i*-C_4H_{10} (Nanjing, 99.99%), *n*-C_5H_{12} (Nanjing, 99.99%), *n*-C_6H_{14} (Hangzhou, ⩾99.00%), *n*-C_7H_{16} (Hangzhou, ⩾99.5%), *n*-C_8H_{18} (Shanghai, ⩾99.7%). All gases were degassed by repeated freeze–pump–thaw cycles in liquid nitrogen. Ar (Nanjing gas 99.999%) was used without further purification.

3. Results and discussion

3.1. Kinetics description

In order to keep the concentration of C_2 ($a^3\Pi_u$) radical constant, the concentrations of precursor, the total pressure (circa 15 Torr), and the delay time between the photolysis laser and the pump laser were kept constant in all experiments. The typical time-resolved fluorescence decay signal of C_2 ($d^3\Pi_g$) being quenched by heptane is illustrated in Fig. 1a. The semi-logarithmic plots in Fig. 1b demonstrate the nature of the exponential decays. The solid line is the result of liner least squares fit corresponding to more than a 60 ns delay from the maximum point to reduce the disturbance caused by laser scattering light. The plots clearly show a single exponential decay curve. The experimentally monitored decay was fitted to

$$I = I_0 \exp(-k't), \tag{1}$$

where k' is the pseudo-first-order rate coefficient. The values of k' at different partial pressure of quencher were derived from similar plots as those illustrated in Fig. 1. The first-order rate coefficient k' is accounting for the quenching of C_2 ($d^3\Pi_g$) by quenchers (k_q) and background gases (k_i), and the Einstein spontaneous emission of C_2 (k_f). In this type of reaction system, background gases include Ar, precursor and some

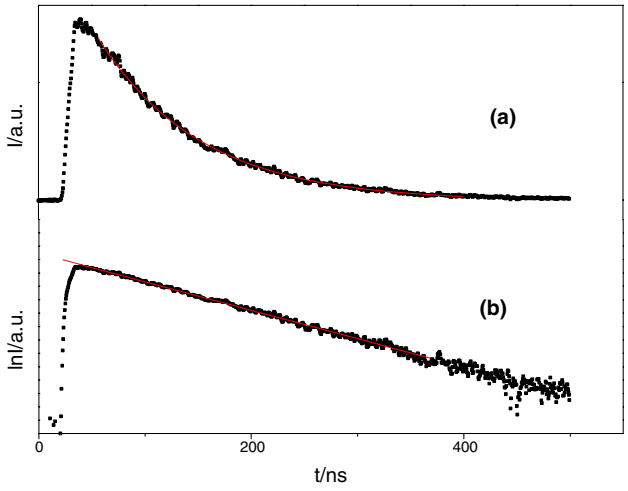

Fig. 1. A typical time-resolved fluorescence decay signal of C_2 ($d^3\Pi_g$) being quenched by heptane. Concentrations are 2.5×10^{14} molecule cm^{-3} and 9×10^{14} molecule cm^{-3} for C_2Cl_4 and heptane, respectively. Plot (a) and its semi-logarithmic plot (b) at 516.5 nm: (.) experimental data and (—) fitting result.

fragments of photolysis. Therefore, the first-order rate coefficient k' should be expressed as

$$k' = k_q[C] + \sum_i k_i[M_i] + k_f. \quad (2)$$

In present case, the background gases and total pressure were constant, so the first-order rate coefficient k' increased proportionally to the concentration of the added quenchers, as illustrated in Fig. 2. The quenching rate constants k_q were obtained by linear least-square fitting according to Eq. (2) from those plots as shown Fig. 2. In addition the averaged collision cross sections σ_q were also obtained. The rate constants k_q and averaged collision cross sections σ_q for collision quenching of C_2 ($d^3\Pi_g$) by the selected alkanes and substituted methane at 298 K are summarized in Table 1.

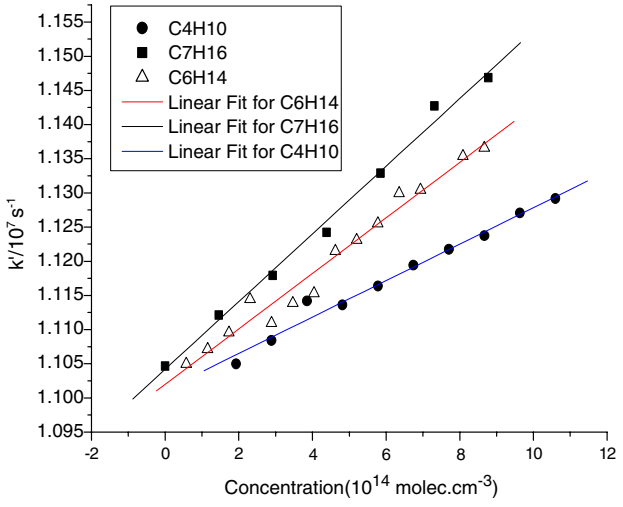

Fig. 2. Plot of the first-order rate constant k' for quenching of C_2 ($d^3\Pi_g$) as a function of concentration of C_4H_{10}, C_6H_{14} and C_7H_{16}.

Table 1
The summary of the quenching rate constants k_q and cross sections σ_q of C_2 ($d^3\Pi_g$) radicals by alkanes and substituted methane molecules measured at 298 K

Quencher	k_q (10^{-10} cm^3 molecule^{-1} s^{-1})	σ_q (10^{-2} nm^2)
CH_4	0.37 ± 0.014	5.44 ± 0.21
C_2H_6	0.57 ± 0.028	8.40 ± 0.41
C_3H_8	0.84 ± 0.033	12.4 ± 0.49
n-C_4H_{10}	2.52 ± 0.082	37.2 ± 1.22
i-C_4H_{10}	1.81 ± 0.11	26.8 ± 1.57
n-C_5H_{12}	3.68 ± 0.17	54.3 ± 2.48
n-C_6H_{14}	4.06 ± 0.195	60.0 ± 2.87
n-C_7H_{16}	4.51 ± 0.16	66.6 ± 2.42
n-C_8H_{18}	4.70 ± 0.17	69.4 ± 2.55
CH_2Cl_2	0.67 ± 0.024	9.87 ± 0.35
$CHCl_3$	0.82 ± 0.043	12.2 ± 0.64
CCl_4	1.23 ± 0.041	8.1 ± 0.61

3.2. Quenching of C_2 ($d^3\Pi_g$) by alkane

It is shown that the quenching rate constants and collision cross sections of C_2 ($d^3\Pi_g$) by alkane increase steadily with the increasing number of C–H bonds contained in the alkane. The quenching of the electronically excited C_2 ($d^3\Pi_g$) radical is a complicated process, including not only physical quenching but also chemical reaction. Although we cannot obtain the precise mechanism only depending on the collision rate constants of C_2 ($d^3\Pi_g$), we may achieve some reasonable conclusions by qualitative analysis. As for the physical quenching, since alkane molecules are polyatomic molecules, they have multiple normal modes and are easy to energy transfer when colliding with other molecules. The increasing number of normal modes accompanying with the increase of the number of carbon atoms in alkane molecules leads to the higher state density and probability of energy transfer. On the other hand, the C–H bonds in alkane molecules have an essentially similar reactivity without taking into account the effect of spatial resistance. So, the collision cross sections increase with the increasing number of C–H bonds. All of these factors could qualitatively explain the trend of our experimental results. The dependence of the collision cross sections on the number of C–H bonds contained in the alkane molecules is shown in Fig. 3.

3.3. Quenching of C_2 ($d^3\Pi_g$) by substituted methane

It is shown in Table 1 that the collision quenching rates of C_2 ($d^3\Pi_g$) by the substituted methane, as well as the cross sections, are all bigger than that of C_2 ($d^3\Pi_g$) by CH_4. We can also find from Table 1 that the collision quenching rates of C_2 ($d^3\Pi_g$) by $CHCl_3$ is

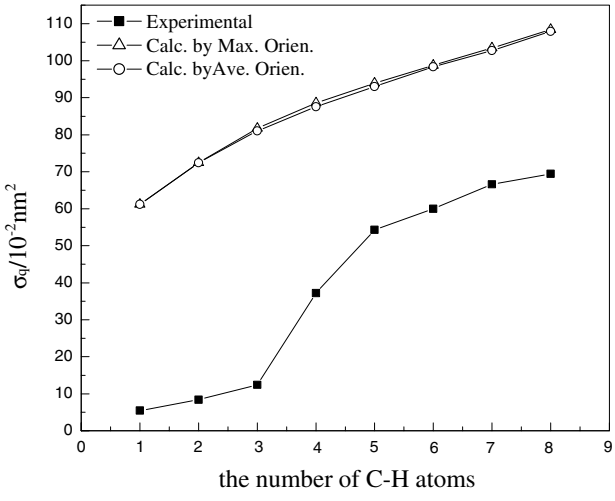

Fig. 3. The dependence of the experimental cross sections, σ_q for quenching of C_2 ($d^3\Pi_g$) by alkanes on the number of C–H atoms in the alkane molecules.

larger than that of CH_2Cl_2 molecule. This is probably because the polarity of C–Cl bond is stronger than that of C–H bond, and furthermore, the volume of Cl atom is bigger than that of H atom. Therefore, the attractive force between C_2 ($d^3\Pi_g$) and chlorine substituting methane is stronger than that between C_2 ($d^3\Pi_g$) and methane when the C_2 ($d^3\Pi_g$) is closed to the collision partner.

3.4. Comparison with the results calculated using the collision complex model

Some attempts have been made to theoretically characterize the collision-induced electronic quenching that occurs in small molecules [24–27]. In order to obtain insight into the quench mechanism between the selected collision partners and C_2 ($d^3\Pi_g$), we calculated the formation cross sections of the radical adducts of C_2 ($d^3\Pi_g$) with alkanes and substituted methane molecules using the collision complex model proposed by Fairchild et al. [28]. According to this theory, the long range part of the interaction between the C_2 ($d^3\Pi_g$) and alkanes or substituted methane molecules is composed of a sum of attractive multipole interactions (dipole–dipole, dipole–quadrupole, dipole-induced-dipole, and the dispersion) and a repulsive centrifugal barrier. Thus, the effective potential in the collision process could be expressed using the most favorable orientation method as:

$$V_{\text{eff}}(r) = \frac{Eb^2}{r^2} - \frac{C_3}{r^3} - \frac{C_4}{r^4} - \frac{C_6'}{r^6} - \frac{C_6''}{r^6} \tag{3}$$

or the averaged orientation method [29]:

$$V_{\text{eff}}(r) = \frac{Eb^2}{r^2} - \frac{C_6'}{r^6} - \frac{C_8'}{r^6}. \tag{4}$$

The C_n coefficients may be expressed in terms of the dipole and quadrupole moments, polarizability and ionization potential of the excited C_2 and its collision partner. In collision at a particular kinetic energy E, there exists an impact parameter b_0 where the maximum of the effective potential is just equal to E. For $b < b_0$, the barrier will be lower and the collision pair can form a complex. For $b > b_0$, the barrier is higher than E, and the collision pair cannot surmount it and form a complex. So, the cross section for complex formation at this kinetic energy can be expressed as

$$\sigma'_{\text{eff}}(E) = \pi b_0^2(E). \tag{5}$$

Then, the thermally averaged complex formation cross section at temperature T is

$$\sigma'_{\text{eff}}(T) = (1/kT)^2 \int_0^\infty \sigma'_{\text{eff}}(e)\exp(-E/kT)\mathrm{d}E. \tag{6}$$

In the case of a single attractive term, the equations may be solved analytically. The b_0 may be evaluated and then be used with Eqs. (5) and (6) to obtain $\sigma_{\text{eff}}(T)$. The quadrupole moment and the polarizability are estimated by N_2. These necessary approximations are reasonable because the same values are used for each collision partner. The results of the calculations at 298 K, the parameters used in the calculations, and the experimentally measured quenching cross sections are summarized in Table 2.

According to the collision complex model of Fairchild [28], the cross section for quenching is that for complex formation times a probability p that quenching will occur during the residence time of the complex, via $\sigma_q = p\sigma_{\text{eff}}$. Table 2 lists the P values for the alkane molecules and substituted methane molecules. The experimentally measured quenching cross sections σ_q are in qualitative agreement with the calculated formation cross section σ_{eff}. They both increased with the increasing number of C–H bonds in the molecules. For substituted methane molecules, the σ_{eff}, as well as the σ_q, is generally larger than that for methane molecules. This

Table 2
Summary of the measured quenching rate constants, σ_q, the calculated formation cross sections σ_{eff} (10^{-2} nm^2) and the parameters used in the calculations at 298 K

Quencher	μ[a] (Debye)	α[a] (Å^3)	Q[b] (10^{-26} ecu . cm^2)	I.P.[a] (eV)	σ_q (10^{-2} nm^2)	Max.[c]		Ave.[d]	
						σ_{eff}	P	σ_{eff}	P
CH_4	0.00	2.59	0.00	12.61	5.44 ± 0.21	61.22	0.089	61.22	0.089
C_2H_6	0.00	4.47	0.65	11.50	8.40 ± 0.41	72.43	0.12	72.43	0.12
C_3H_8	0.08	6.37	1.50	11.10	12.4 ± 0.49	81.76	0.15	81.07	0.15
n-C_4H_{10}	0.03	8.20	2.00	10.63	37.2 ± 1.22	88.56	0.42	87.55	0.43
n-C_5H_{12}	0.13	9.99	2.60	10.28	54.3 ± 2.48	93.93	0.58	93.04	0.58
n-C_6H_{14}	0.05	11.9	3.00	10.13	60.0 ± 2.87	98.72	0.61	98.38	0.61
n-C_7H_{16}	0.10	13.7	3.50	9.93	66.6 ± 2.42	103.43	0.64	102.78	0.65
n-C_8H_{18}	0.08	15.9	3.90	9.80	69.4 ± 2.55	108.41	0.64	107.9	0.64
CH_2Cl_2	1.60	6.48	4.10	11.32	9.87 ± 0.35	95.80	0.103	84.07	0.117
$CHCl_3$	1.04	9.5	3.50	11.37	12.2 ± 0.64	100.82	0.121	93.69	0.130
CCl_4	0.00	11.2	0.00	11.47	18.1 ± 0.61	98.34	0.184	98.34	0.184

[a] Ref. [30].
[b] Refs. [31,23].
[c] Calculated using the most favorable orientation method.
[d] Calculated using the averaged orientation method.

comparison of experimental and calculated cross sections can only be viewed as guidance as to the mechanism of quenching. This simple one-dimensional collision calculation is a very approximate version of the actual dynamics of such complex formation. The approximation was made of a separate σ_{eff} calculated for each component of the interaction, with the total σ_{eff} taken as the sum of those cross sections. In fact, the various interactions are often of comparable magnitude, necessitating the numerical computation. It is therefore suggested that this comparison is more qualitatively applicable than quantitatively. From the comparison, it could be concluded that the attractive forces and collision complex formation play an important role in the collision quenching of C_2 ($d^3\Pi_g$) by selected collision partners.

Acknowledgments

This work was financially supported by the China National Key Basic Research Special Foundation (G1999075304), the China National Natural Science Foundation (20373065, 20328305), and Chinese Academy of science (KJCX2-SW-H08).

References

[1] A. Mckellar, J. Roy. Astron. Soc. Can. 54 (1960) 97.
[2] D.L. Lambert, E.A. Mallia, Bull. Astr. Inst. Czechoslovakia. 25 (1974) 216.
[3] F.H. Chaffee Jr., B.L. Lutz, J.H. Black, P.A. Vanden Bout, R.L. Snell, Astrophys. J. 236 (1980) 474.
[4] A.C. Danks, D.L. Lambert, Astrophys. J. 124 (1983) 188.
[5] J.D. Campbell, M.H. Yu, M. Mangir, C. Wittig, J. Chem. Phys. 69 (1978) 3854.
[6] H. Reisler, M. Mangir, C. Wittig, Chem. Phys. 47 (1980) 49.
[7] H. Reisler, M. Mangir, C. Wittig, J. Chem. Phys. 71 (1979) 2109.
[8] M.S. Mangir, H. Reisler, C. Wittig, J. Chem. Phys. 73 (1980) 829.
[9] H. Reisler, M.S. Mangir, C. Wittig, J. Chem. Phys. 73 (1980) 2280.
[10] L. Pasternack, W.M. Pitts, J.R. McDonald, Chem. Phys. 57 (1981) 19.
[11] L. Pasternack, A.P. Baronavski, J.R. McDonald, J. Chem. Phys. 73 (1980) 3508.
[12] W.M. Pitts, L. Pasternack, J.R. McDonald, Chem. Phys. 68 (1982) 417.
[13] A. Ristanovic, A. Fernandez, A. Fontijin, J. Phys. Chem. A 106 (2002) 8291.
[14] A. Fontijin, A. Fernandez, A. Ristanovic, M.Y. Randall, J.T. Jankowiak, J. Phys. Chem. A 105 (2001) 3182.
[15] R.I. Kaiser, M. Yamada, Y. Osamura, J. Phys. Chem. A 106 (2002) 4825.
[16] N. Balucani, A.M. Mebel, Y.T. Lee, R.I. Kaiser, J. Phys. Chem. A 105 (2001) 9813.
[17] J. Wang, K. Han, G. He, Z. Li, V.R. Morris, J. Phys. Chem. A 107 (2003) 9825.
[18] J. Wang, K. Han, G. He, Z. Li, Chem. Phys. Lett. 368 (2003) 139.
[19] C.S. Huang, Z.Q. Zhu, Y. Xin, L.S. Pei, C.X. Chen, Y. Chen, J. Chem. Phys. 120 (2004) 2225.
[20] C.S. Huang, Z.X. Li, D.F. Zhao, Y. Xin, L.S. Pei, C.X. Chen, Y. Chen, Chinese Sci. Bull. 49 (2004) 120.
[21] C.S. Huang, D.F. Zhao, L.S. Pei, C.X. Chen, Y. Chen, Chem. Phys. Lett. 389 (2004) 230.
[22] H. Geiger, P. Wiesen, K.H. Becker, Phys. Chem. Chem. Phys. 1 (1999) 5601.
[23] Y. Gao, Y. Chen, X. Ma, C. Chen, Chem. Phys. 269 (2001) 389.
[24] C.A. Thayer, J.T. Yardley, J. Chem. Phys. 57 (1972) 3992.
[25] H.M. Lin, M. Seaver, K.Y. Tang, A.E. Knight, C.S. Parmenter, J. Chem. Phys. 70 (1979) 5442.
[26] F.W. Byron, H.M. Foley, Phys. Rev. A 134 (1964) 625.
[27] J.E. Selwyn, J.I. Steinfeld, Chem. Phys. Lett. 4 (1969) 217.
[28] P.W. Fairchild, G.P. Smith, D.R. Crosley, J. Chem. Phys. 79 (1983) 1795.
[29] J.O. Hirschfelder, C.F. Curtiss, R.B. Bird, Molecular Theory of Gases and Liquids, Wiley, New York, 1954.
[30] D.R. Lide, CRC Handbook of Chemistry and Physics, 80th edn., CRC, Boca Raton, FL, 1999–2000 (chapter 9).
[31] C.J. Nokes, R.J. Donvan, Chem. Phys. 90 (1989) 167.